Capacity Analysis of Multi-Pair Orbital Angular Momentum Interference Networks

Woong Son[1], Howon Lee[2], and Bang Chul Jung[1]
[1]Dept. of Electronics Engineering, Chungnam National University, Daejeon 34134, Republic of Korea,
[2]Dept. of EECE and IITC, Hankyong National University, Anseong, Gyeonggi 17579, Republic of Korea,
Email: {woongson, bcjung}[1]@cnu.ac.kr, hwlee[2]@hknu.ac.kr

***Abstract*—In this paper, we investigate a multi-pair *orbital angular momentum* (OAM) interference network adopting mode-division multiplexing (MDM) at each transmitter, where multiple transmitter–receiver pairs exploit the same multiple OAM modes. Even though many previous studies on the OAM-MDM exist in literature, they only focused on a single transmitter–receiver pair and did not consider the inter-pair interference. In practice, wireless fronthaul and backhaul links reuse the same frequency band and they may interfere with each other. We first mathematically characterize the Laguerre-Gaussian (LG) beam-based OAM wireless channel and then analyze the channel capacity of the multi-pair OAM interference channel. It is worth noting that this is the first theoretical result in literature. Through extensive computer simulations, we validate the channel capacity of the multi-pair OAM-MDM interference channel by considering the interference among different OAM beams according to various system parameters such as the number of OAM modes, the distance between the transmitter and receiver, the distance between adjacent transmit antennas, the waist of the OAM beams, etc.**

***Index Terms*—Orbital angular momentum (OAM), mode-division multiplexing (MDM), Laguerre-Gaussian (LG) beam, interference channel, channel capacity.**

I. Introduction

Line-of-sight (LoS) wireless communications between fixed base stations (BSs) have received much interest from both industry and academia for future high capacity point-to-point (P2P) communication systems especially over 100 GHz frequency bands [1]. Different from the communication scenario in rich scattering environments, multiple input multiple output (MIMO) technique needs to be carefully designed to provide the additional spatial degrees of freedom and improve data rates since the channel responses becomes highly correlated each other in the LoS environment, leading to the MIMO channel of rank 1 [2]. Recently, an orbital angular momentum (OAM)-based communication has been considered as one of the most promising technologies for the LoS communication scenario [3]–[5]. The OAM technique can effectively send multiple independent signals over different (orthogonal) modes even in the LoS wireless channel and thus it increases the transmission rate in a P2P wireless link such as wireless backhaul and/or fronthaul [6]. In theory, signals received via different OAM modes are mutually orthogonal, assuming the coaxially aligned transmitter and receiver pair.

In particular, a single transmitter and receiver pair OAM-*mode-division multiplexing* (MDM) communication system based on Laguerre-Gaussian (LG) beam was implemented in millimeter-wave (mm-wave) carrier frequency 28 GHz band [4]. In the OAM-MDM communication system, the transmit aperture multiplexes multiple independent data signals via different OAM modes which are mutually orthogonal to each other and it was shown that 32 Gbps data-rate can be achieved. Another single transmitter and receiver pair OAM-MDM communication system with the LG beam was experimentally investigated, while the OAM-MDM was mathematically analyzed in terms of communcation capacity [7]. An MIMO OAM-MDM system was proposed and implemented by using a spiral phase plate (SPP) to generate the OAM wave, where the OAM-MDM and the conventional spatial multiplexing are combined for a single transmitter and receiver pair [8]. Another MIMO OAM-MDM system was proposed and implemented by using uniform circular array (UCA) in a 28 GHz frequency band [9], where 100 Gbps of data rate was achieved at 10 [m] communication distance[1]. In addition, a novel transmission technique that combines a spatial modulation and the OAM-MDM was proposed in [10], where the proposed technique was analyzed in terms of achievable rate, average bit error rate (BER), and energy efficiency (EE). In [11], the OAM wireless channel was characterized by considering the spatial energy distribution of the OAM waves. Unlike previous OAM communication studies considering radio frequency, there is also a study analyzing BER and channel capacity in OAM-MIMO system in a single optical link under atmospheric turbulence [12].

Even though many studies on the OAM-MDM and the MIMO OAM-MDM have been performed for a single transmitter and receiver par in literature, the interference among multiple pairs adopting OAM-based communication techniques has not been investigated so far. In general, the interference is one of the most critical factors to deteriorate performances of wireless communication systems. Hence, we investigate a multi-pair MDM system using mmwave OAM, where multiple transmitter and receiver pairs exploit the same multiple OAM modes in this paper.

The remainder of this paper is organized as follows. Section II describes system and channel model of the multi-pair

[1]The authors of [9] used different terminology from ours. They call OAM multiplexing the OAM-MDM of this paper, and they call OAM-MIMO the MIMO OAM-MDM of this paper. In fact, the terminologies regarding the various OAM systems were not clear in literature since many researchers have defined them in their own way.

978-1-7281-0960-2/19/$31.00 ©2019 IEEE

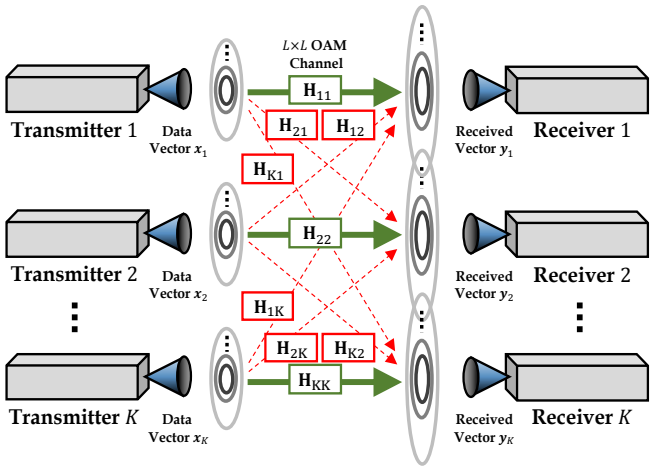

Fig. 1: System model of the multi-pair OAM-MDM interference channel.

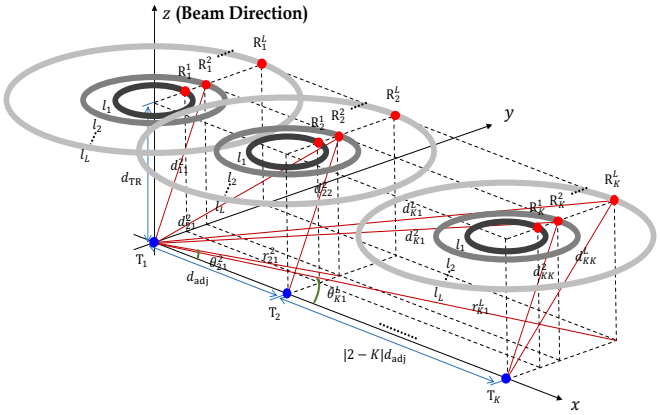

Fig. 2: Transmit and receiver antenna positioning in cylindrical coordinate system.

OAM-MDM systems. In Section III, the channel capacity is analyzed of the multi-pair OAM-MDM systems. In Section IV, numerical examples are shown via extensive computer simulations and conclusions are drawn in Section V.

II. System and OAM Channel Model

A. System Model

First, we explain a system model of the K-pair OAM-MDM interference channel consisting of perfectly aligned K transmitters and K corresponded receivers. A transmit antenna at each transmitter can generate L OAM signals with different OAM modes. So the set of OAM modes denotes $\mathcal{L} \triangleq \{l_1, l_2, ..., l_m, ..., l_L\}$ and the m-th OAM mode from each transmitter denotes l_m, where $m \in \{1, 2, ..., L\}$. Correspondingly, each receiver is equipped with L antennas for L OAM signals reception. Then, the OAM channel matrix from the j-th transmitter to the i-th receiver $\mathbf{H}_{ij} \in \mathbb{C}^{L\times L}$ is given as

$$\mathbf{H}_{ij} = \begin{bmatrix} h_{ij}^{11} & h_{ij}^{12} & \cdots & h_{ij}^{1m} & \cdots & h_{ij}^{1L} \\ h_{ij}^{21} & h_{ij}^{22} & \cdots & h_{ij}^{2m} & \cdots & h_{ij}^{2L} \\ \vdots & \vdots & \ddots & \vdots & \ddots & \vdots \\ h_{ij}^{n1} & h_{ij}^{n2} & \cdots & h_{ij}^{nm} & \cdots & h_{ij}^{nL} \\ \vdots & \vdots & \ddots & \vdots & \ddots & \vdots \\ h_{ij}^{L1} & h_{ij}^{L2} & \cdots & h_{ij}^{Lm} & \cdots & h_{ij}^{LL} \end{bmatrix}, \quad (1)$$

where the $i, j \in \{1, 2, ..., K\}$ and $n \in \{1, 2, ..., L\}$. The $h_{ij}^{nm} \in \mathbb{C}$ denotes the OAM channel transfer via the m-th OAM signal from the j-th transmit antenna to the n-th receive antenna at the i-th receiver. The OAM channel characterization based on geometrical and LG beam parameter is explained in next subsection II-B in detail.

In addition, the data vector from the j-th transmitter is represented as $\mathbf{x}_j = [x_{1j}, x_{2j}, ..., x_{mj}, ..., x_{Lj}]^T \in \mathbb{C}^{L\times 1}$ and the power constraint $\mathbb{E}\left[||\mathbf{x}_j||^2\right] = P$ is satisfied for all j. Without any loss of generality, the received signal vector at the i-th receiver $\mathbf{y}_i = [y_{1i}, y_{2i}, ..., y_{ni}, ..., y_{Li}]^T \in \mathbb{C}^{L\times 1}$ can be represented as

$$\mathbf{y}_i = \sum_{j=1}^{K} \mathbf{H}_{ij}\mathbf{x}_j + \mathbf{n}_i, \quad (2)$$

where the additive white Gaussian noise (AWGN) vector at the i-th receiver is denoted as $\mathbf{n}_i = [n_{1i}, n_{2i}, ..., n_{ni}, ..., n_{Li}]^T \in \mathbb{C}^{L\times 1}$ and each component is circular symmetric complex white Gaussian noise with $\mathcal{CN}(0, N_0)$.

B. OAM Channel Model

We characterize the LG beam based OAM channel in this subsection. In cylindrical coordinate system with (r, ϕ, z), the beam waist of the m-th OAM signal on the plane z denotes $w(z) = w_0\sqrt{1 + (z/z_R)^2}$, where the beam waist of the OAM signal on the plane $z = 0$ is w_0. In addition, the Rayleigh distance of the m-th OAM signal denotes $z_R = \pi w_0^2/\lambda$, where the wave length is given by λ which corresponds to the carrier frequency. Thus, when the w_0 is determined, the $w(z)$ and z_R can be sequentially calculated, respectively. When a transmit antenna located at the origin $(0, 0, 0)$ in cylindrical coordinate system and radiates to the positive direction of z-axis, the generalized LG beam $u_{p,l_m}(r, \phi, z)$ can be represented as Eq. (3), where the normalized constant is $\alpha\sqrt{\frac{p!}{\pi(p+|l_m|)!}}$ and the $L_p^{|l_m|}(\cdot)$ is the Laguerre polynomial.

On the other hands, we explain the position of transmit antennas and receive antennas in cylindrical coordinate system in detail. We assume that all receive antennas are located on the plane $z = d_{\mathsf{TR}}$. The first transmit antenna position denotes origin $(0, 0, 0)$. Also the position of the j-th transmit antenna denotes $(|j-1|d_{\mathsf{adj}}, 0, 0)$ for all j, where the relative distance between adjacent transmit antennas is d_{adj} [m]. In addition, the relative coordinates of the n-th receive antenna at the i-th receiver from the first transmit antenna (the origin in cylindrical coordinate system) is denoted by $(r_{i1}^n, \phi_{i1}^n, d_{\mathsf{TR}})$. Also the position of the n-th receive antenna at the i-th receiver from the j-th transmit antenna is denoted by $(r_{ij}^n, \phi_{ij}^n, d_{\mathsf{TR}})$ Similarly, when each transmit antenna's the position are assumed to be origin, the relative radial position and transverse

$$u_{p,l_m}(r,\phi,z) = \alpha\sqrt{\frac{p!}{\pi(p+|l_m|)!}}\frac{1}{w(z)}\left(\frac{r\sqrt{2}}{w(z)}\right)^{|l_m|}\exp\left(-\left(\frac{r}{w(z)}\right)^2\right)L_p^{|l_m|}\left(\frac{2r^2}{w^2(z)}\right) \times \exp\left(-\frac{i\pi r^2}{\lambda z\left(1+\left(\frac{\pi w^2(z)}{\lambda z}\right)^2\right)}\right)\exp\left(i\left(|l_m|+2p+1\right)\arctan\left(\frac{z}{z_R}\right)\right)\exp\left(-il_m\phi\right), \tag{3}$$

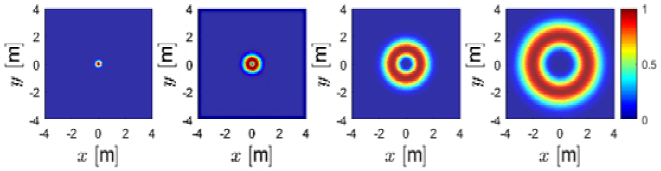

Fig. 3: Example of the normalized LG beam based OAM channel intensity distribution on focal plane. (Left to right, OAM mode $0, +1, +3$ and $+5$)

azimuthal angle from the j-th transmit antenna to the n-th receive antenna at the i-th receiver r_{ij}^n and ϕ_{ij}^n for all receive antennas at receivers can be defined as

$$r_{ij}^n = \sqrt{\left(|j-i|d_{\mathsf{adj}}\right)^2 + r_{\mathsf{max}}^2(d_{\mathsf{TR}}, l_m)}, \tag{4}$$

$$\phi_{ij}^n = \begin{cases} \arctan\frac{r_{\mathsf{max}}(d_{\mathsf{TR}},l_m)}{|j-i|d_{\mathsf{adj}}} & i > j \\ \pi/2 & i = j \\ \pi - \arctan\frac{r_{\mathsf{max}}(d_{\mathsf{TR}},l_m)}{|j-i|d_{\mathsf{adj}}} & i < j. \end{cases} \tag{5}$$

Correspondingly, the relative distance from the j-th transmit antenna to the n-th receive antenna at the i-th receiver can be calculated as

$$d_{ij}^n = \sqrt{(|j-i|d_{\mathsf{adj}})^2 + r_{\mathsf{max}}^2(d_{\mathsf{TR}}, l_m) + d_{\mathsf{TR}}^2}. \tag{6}$$

However, the radius of the maximum energy strength circle on the plane z (red area which close to 1 in Fig. 3) denotes $r_{\mathsf{max}}(z, l_m)$, which is the function of z and l_m. So receiver antennas should be designed positioning on the radius the maximum energy strength circle on the plane $z = d_{\mathsf{TR}}$ for maximizing desired channel intensity, where the relative distance from the transmitter and receiver d_{TR}. Considering the radius of the maximum energy strength circle on the plane z, all of corresponded receive antennas' positions with each transmitter can be designed as

$$r_{\mathsf{max}}(d_{\mathsf{TR}}, l_m) = \sqrt{\frac{|l_m|}{2}}w(d_{\mathsf{TR}}). \tag{7}$$

Now, we explain the LG beam based OAM channel transfer. At first, we consider the OAM channel between a non-pair transceiver when $i \neq j$ case. In addition, we also assumed to be $z = d_{\mathsf{TR}}$. Then, the OAM channel transfer via the m-th OAM signal from the j-th transmit antenna to the n-th receive antenna at the i-th receiver h_{ij}^{nm} is given as

$$h_{ij}^{nm} = \mathcal{B}_{ij}^{nm}\frac{\lambda}{4\pi d_{ij}^n}\exp\left(-ikd_{ij}^n\right)\exp\left(-i\phi_{ij}^n l_m\right), \tag{8}$$

where the wave number is $k = 2\pi/\lambda$ and the OAM channel gain coefficient via the m-th OAM signal from the j-th transmit antenna to the n-th receive antenna at the i-th receiver is $\mathcal{B}_{ij}^{nm}$.

Similarly, we also consider the OAM channel between a pair transceiver when $i = j$ case. The OAM channel transfer via the m-th OAM signal from the j-th transmit antenna to the m-th receive antenna at the j-th receiver h_{jj}^{mm} is given as

$$h_{jj}^{mm} = \mathcal{B}\frac{\lambda}{4\pi d_{jj}^m}\exp\left(-ikd_{jj}^m\right)\exp\left(-i\phi_{jj}^m l_m\right), \tag{9}$$

where the desired OAM channel gain coefficient via the m-th OAM signal from the j-th transmit antenna to the m-th receive antenna at the j-th receiver is $\mathcal{B}$.

On the other hands, via the m-th OAM signal from the j-th transmit antenna, the unit step pulse x_{mj} is transmitted to the m-th receive antenna at the j-th receiver, the channel response represents $u_{p,l_m}(r_{jj}^m, \phi_{jj}^m, d_{\mathsf{TR}}) = h_{jj}^{mm}x_{mj}$. In addition, via the m-th OAM signal from the j-th transmit antenna, the unit step pulse x_{mj} is also transmitted to the n-th receive antenna at the i-th receiver, the channel response also represents $u_{p,l_m}(r_{ij}^n, \phi_{ij}^n, d_{\mathsf{TR}}) = h_{ij}^{nm}x_{mj}$. In general, the radial mode p assumed to be 0 in OAM communication systems [11], [13], so $L_p^{|l_m|}(\cdot) = 1$ is simply satisfied for all l_m. Then, when the radial mode p is equal to 0, the relationship is represented by

$$\frac{u_{0,l_m}(r_{ij}^n, \phi_{ij}^n, d_{\mathsf{TR}})}{u_{0,l_m}(r_{jj}^m, \phi_{jj}^m, d_{\mathsf{TR}})} = \frac{h_{ij}^{nm}}{h_{jj}^{mm}}, \tag{10}$$

for all i, j, m and n.

By plugging Eq. (3), (8) and (9) into Eq. (10), the left-hand and right-hand side of Eq. (10) are given as Eq. (11) and (12), respectively. Thus, the OAM channel matrix from the j-th transmitter to the i-th receiver $\mathbf{H}_{ij}$ in Eq. (1) can be attained by using Eq. (13), for all i and j.

III. Channel Capacity of the Multi-pair OAM-MDM Interference Channel

A multi-pair OAM-MDM interference channel is fundamentally the same a multi-user MIMO interference channel, the total channel capacity [14] based on Eq. (1) is given by Eq. (14), where the additive white Gaussian noise variance at each receive antenna is N_0.

IV. Simulation Results

In this section, via computer simulations, we evaluate the channel capacity of the multi-pair OAM-MDM interference channel according to various system parameters, such as the

$$\frac{u_{0,l_m}(r_{ij}^n,\phi_{ij}^n,d_{\mathsf{TR}})}{u_{0,l_m}(r_{jj}^m,\phi_{jj}^m,d_{\mathsf{TR}})}=\left(\frac{r_{ij}^n}{r_{jj}^m}\right)^{|l_m|}\exp\left(-\frac{\left(r_{ij}^n\right)^2-\left(r_{jj}^m\right)^2}{w^2(d_{\mathsf{TR}})}\right)\exp\left(-\frac{i\pi\left(\left(r_{ij}^n\right)^2-\left(r_{jj}^m\right)^2\right)}{\lambda d_{\mathsf{TR}}\left(1+\left(\frac{\pi w^2(d_{\mathsf{TR}})}{\lambda d_{\mathsf{TR}}}\right)^2\right)}\right). \tag{11}$$

$$\frac{h_{ij}^{nm}}{h_{jj}^{mm}}=\frac{\mathcal{B}_{ij}^m}{\mathcal{B}}\frac{d_{jj}^m}{d_{ij}^n}\exp\left(-ik\left(d_{ij}^n-d_{jj}^m\right)\right)\exp\left(-il_m\left(\phi_{ij}^n-\phi_{jj}^m\right)\right). \tag{12}$$

$$h_{ij}^{nm}=\mathcal{B}\frac{\lambda}{4\pi d_{jj}^m}\left(\frac{r_{ij}^n}{r_{jj}^m}\right)^{|l_m|}\exp\left(-\frac{\left(r_{ij}^n\right)^2-\left(r_{jj}^m\right)^2}{w^2\left(d_{\mathsf{TR}}\right)}\right)\exp\left(-\frac{i\pi\left(\left(r_{ij}^n\right)^2-\left(r_{jj}^m\right)^2\right)}{\lambda d_{\mathsf{TR}}\left(1+\left(\frac{\pi w^2(d_{\mathsf{TR}})}{\lambda d_{\mathsf{TR}}}\right)^2\right)}\right)\exp\left(-ikd_{jj}^m\right)\exp\left(-i\phi_{ij}^n l_m\right). \tag{13}$$

$$C_{\mathsf{total}}=\sum_{i=1}^{K}\mathbb{E}\left(\log_2\left(\det\left(\mathbf{I}_L+\frac{1}{N_0}\mathbf{H}_{ii}\mathbf{H}_{ii}^H\left(\mathbf{I}_L+\sum_{j\neq i}^{K}\frac{1}{N_0}\mathbf{H}_{ij}\mathbf{H}_{ij}^H\right)^{-1}\right)\right)\right), \tag{14}$$

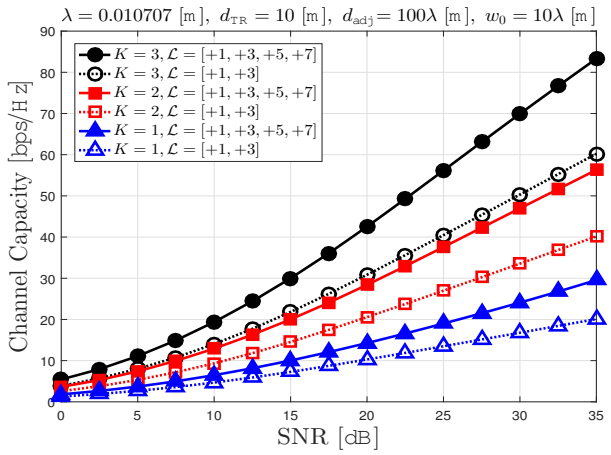

Fig. 4: Channel capacity with respect to the received SNR.

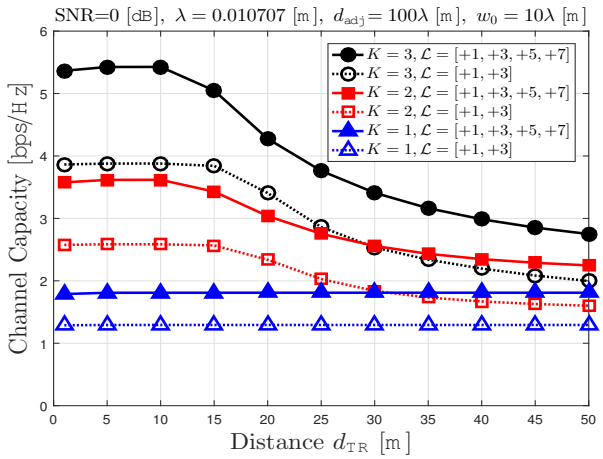

Fig. 5: Channel capacity with respect to the relative distance between a transceiver.

number of OAM modes, relative distance between transceiver, relative distance between adjacent transmit antennas and beam waist of OAM beams. We assume the carrier frequency is equal to 28 GHz and the wave length λ is correspondingly equal to 0.010707 [m]. Before the evaluation of results, we explain some notation as follows. The set $\mathcal{L}=[+1,+3,+5,+7]$ represents the four $(+1,+3,+5,+7)$ OAM modes which are simultaneously radiated at each transmit antenna. The first, second, third and fourth OAM mode represent the $+1,+3,+5$ and $+7$, respectively. In addition, the relative distance between transceiver and the relative distance between adjacent transmit antennas are represented as d_{TR} [m] and d_{adj} [m], respectively. The beam waist of OAM signals on plane $z=0$ denotes w_0 [m].

Fig. 4 shows that the channel capacity of the K-pair OAM-MDM interference channel according to the received SNR via the first OAM signal from the j-th transmit antenna to the first receive antenna at the j-th receiver when the relative distance between a transceiver $d_{\mathsf{TR}}=10$ [m], the relative distance between transmit antennas $d_{\mathsf{adj}}=100\lambda$ [m] and the beam waist $w_0=10\lambda$ [m]. In general, when the relative distance between transmit antennas d_{adj} is enough large 100λ [m] and the relative distance between a transceiver d_{TR} is 10 [m] for all K case, the channel capacity increases according to received SNR due to very small interference between transceivers. As the number of transceivers K increases, the channel capacity increases as well. Furthermore, the number of OAM modes increases from two ($\mathcal{L}=[+1,+3]$) to four ($\mathcal{L}=[+1,+3,+5,+7]$), the channel capacity also increases due to the increased multiplexing gain.

Fig. 5 shows that the channel capacity of the K-pair OAM-MDM interference channel according to the relative distance between a transceiver d_{TR} when the received SNR via the first OAM signal from the j-th transmit antenna to the first receive antenna at the j-th receiver is 0 [dB], the relative distance between transmit antennas $d_{\mathsf{adj}}=100\lambda$ [m] and the beam waist $w_0=10\lambda$ [m]. In $K=1$ case, the channel capacity does not depend on the relative distance between a transceiver d_{TR} since there is no inter-pair interference. However, the channel capacity in $K\geq 2$ cases, as the relative distance between a transceiver d_{TR} increases, the beam waist on plane z also increases. Therefore, as the inter-pair interference increases, the channel capacity decreases.

Fig. 6 shows that the channel capacity of the K-pair OAM-MDM interference channel according to the relative distance between adjacent transmit antennas d_{adj} when the received SNR via the first OAM signal from the j-th transmit antenna to the first receive antenna at the j-th receiver is 0 [dB], the relative distance between a transceiver $d_{\mathsf{TR}}=10$ [m] and the beam

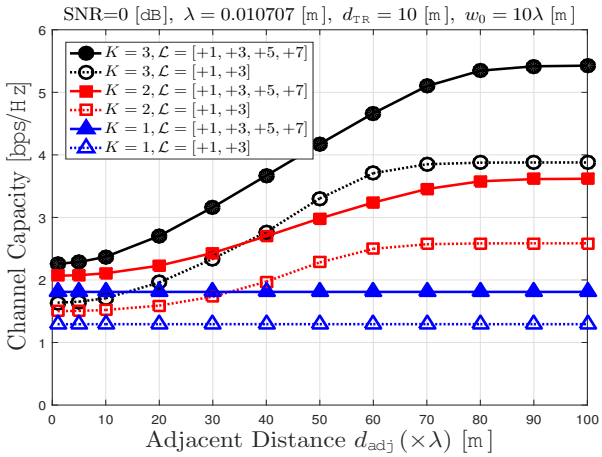

Fig. 6: Channel capacity with respect to the relative distance between adjacent transmit antennas.

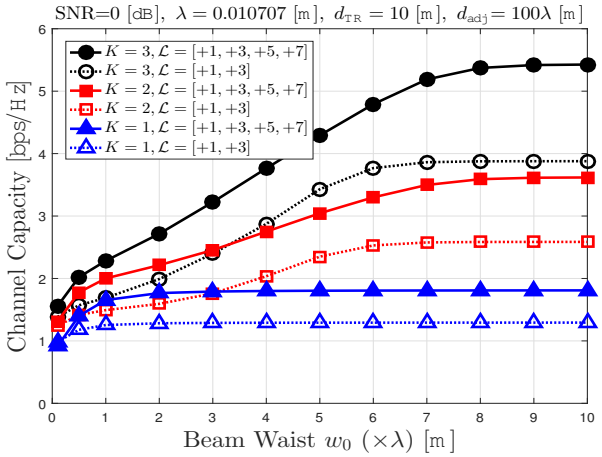

Fig. 7: Channel capacity with respect to the beam waist.

waist of the first OAM signal $w_0 = 10\lambda$ [m]. The $K = 1$ case do not depend on the adjacent transmit antennas d_{adj}, however, we considered in Fig. 6 for comparison with $K \geq 2$ cases. In $K \geq 2$ case, as the relative distance between transmit antennas d_{adj} increases, the channel capacity also increases since inter-pair interference decreases. In particular, when the adjacent distance d_{adj} is enough large, the channel capacity converged a certain value since inter-mode interference (between different OAM modes in pair transceivers) is still existed.

Fig. 7 shows that the channel capacity of the K-pair OAM-MDM interference channel according to the beam waist w_0 when the received SNR via the first OAM signal from the j-th transmit antenna to the first receive antenna at the j-th receiver is 0 [dB], the relative distance between a transceiver $d_{\mathsf{TR}} = 10$ [m] and the adjacent distance between a transmit antennas $d_{\mathsf{adj}} = 100\lambda$ [m]. In general, as the beam waist increases, the channel capacity increases since the Rayleigh distance also increases. If the beam waist is very small, the channel capacity is also small since inter-mode interference can not be ignored. However, even if the beam waist slightly increases, the inter-mode interference is drastically reduced and the channel capacity increases.

V. Conclusion

In this paper, we mathematically characterized the channel capacity of LG beam based OAM-MDM interference networks by considering the effect of interference among multiple OAM transmitter–receiver pairs. Simulation results show the capacity of the multi-pair OAM-MDM interference network according to various system parameters such as the number of OAM modes, relative distance between the transmitter and receiver, relative distance between adjacent transmit antennas, and waist of the OAM beams. The channel capacity becomes increased as the number of modes increases or the distance between adjacent transmitter antennas increases. We leave a practical interference mitigation technique in the multi-pair OAM-MDM interference networks for further study.

Acknowledgment

This work was supported by Samsung Research Funding Center of Samsung Electronics under Project Number SRFC-TB1803-01.

References

[1] C. Koenig, *et al.*, "Wireless sub-THz communication system with high data rate," *Nature Photon.*, vol. 7, no. 12, pp. 977–981, Oct. 2013.

[2] M. H. C. Garcia, M. Iwanow, and R. A. Stirling-Gallacher, "LOS MIMO design based on multiple optimum antenna seperations," in *Proc. IEEE Vehicular Technology Conference (VTC Fall)*, Aug. 2018.

[3] J. Wang, *et al.*, "Terabit free-space data transmission employing orbital angular momentum multiplexing," *Nature Photon.*, vol. 6, pp. 488–496, Jun. 2012.

[4] Y. Yan, *et al.*, "High-capacity millimetre-wave communications with orbital angular momentum multiplexing," *Nature Commun.*, vol. 5, no. 4876, pp. 1–9, Sep. 2014.

[5] I. B. Djordjevic, "Multidimensional OAM-based secure high-speed wireless communications," *IEEE Access*, vol. 5, pp. 16 416–16 428, 2017.

[6] R. M. Henderson, "Let's do the twist!: Radiators, experiments, and techniques to generate twisted waves at radio frequencies," *IEEE Microwave Mag.*, vol. 18, no. 4, pp. 88–96, May 2017.

[7] W. Zhang, *et al.*, "Mode division multiplexing communication using microwave orbital angular momentum: An experimental study," *IEEE Trans. Wireless Commun.*, vol. 16, no. 2, pp. 1308–1318, Feb. 2017.

[8] Y. Ren, *et al.*, "Line-of-sight millimeter-wave communications using orbital angular momentum multiplexing combined with conventional spatial multiplexing," *IEEE Trans. Wireless Commun.*, vol. 16, no. 5, pp. 3151–3161, May 2017.

[9] D. Lee, *et al.*, "An experimental demonstration of 28 GHz band wireless OAM-MIMO (Orbital Angular Momentum Multi-Input and Multi-Output) multiplexing," in *Proc. IEEE Vehicular Technology Conference (VTC Spring)*, Jun. 2018.

[10] X. Ge, R. Zi, X. Xiong, Q. Li, and L. Wang, "Millimeter wave communications with OAM-SM scheme for future mobile networks," *IEEE J. Sel. Areas Commun.*, vol. 35, no. 9, pp. 2163–2177, Sep. 2017.

[11] L. Wang, X. Ge, R. Zi, and C.-X. Wang, "Capacity analysis of orbital angular momentum wireless channels," *IEEE Access*, vol. 5, pp. 23 069–23 077, 2017.

[12] B. B. Yousif, and E. E. Elsayed, "Performance enhancement of an orbital-angular-momentum-multiplexed free-space optical link under atmospheric turbulence effects using spatial-mode multiplexing and hybrid diversity based on adaptive mimo equalization," *IEEE Access*, vol. 7, pp. 84 401–84 412, 2019.

[13] F. Tamburini, E. Mari, A. Sponselli, B. Theide, A. Bianchini, and F. Romanato, "Encoding many channels on the same frequency through radio vorticity: First experimental test," *New, J. Phys.*, vol. 14, Mar. 2012.

[14] R. S. Blum, "MIMO capacity with interference," *IEEE J. Sel. Areas Commun.*, vol. 21, no. 5, pp. 793–801, Jun. 2003.